REVIEW ARTICLE

Physiological limits to life in anoxic subseafloor sediment

William D. Orsi[1,2,*,†], Bernhard Schink[3], Wolfgang Buckel[4] and William F. Martin[5,*]

[1]Department of Earth and Environmental Sciences, Paleontology and Geobiology, Ludwig-Maximilians-Universität München, 80333 Munich, Germany, [2]GeoBio-Center, Ludwig-Maximilians-Universität München, 80333 Munich, Germany, [3]Department of Biology, University of Konstanz, 78457 Constance, Germany, [4]Department of Biology, Philipps-Universität, 35032 Marburg, Germany and [5]Institute for Molecular Evolution, Heinrich Heine Universität Düsseldorf, 40225 Düsseldorf, Germany

*Corresponding author: Universitätsstraße 1, D-40225 Düsseldorf, Germany. Tel: +49 211 81-13011; E-mail: bill@hhu.de and Richard-Wagner Str. 10, Munich Germany 80333. Tel: +49 89 2180 6598 ; E-mail: w.orsi@lrz.uni-muenchen.de

ABSTRACT

In subseafloor sediment, microbial cell densities exponentially decrease with depth into the fermentation zone. Here, we address the classical question of 'why are cells dying faster than they are growing?' from the standpoint of physiology. The stoichiometries of fermentative ATP production and consumption in the fermentation zone place bounds on the conversion of old cell biomass into new. Most fermentable organic matter in deep subseafloor sediment is amino acids from dead cells because cells are mostly protein by weight. Conversion of carbon from fermented dead cell protein into methanogen protein via hydrogenotrophic and acetoclastic methanogenesis occurs at ratios of ∼200:1 and 100:1, respectively, while fermenters can reach conversion ratios approaching 6:1. Amino acid fermentations become thermodynamically more efficient at lower substrate and product concentrations, but the conversion of carbon from dead cell protein into fermenter protein is low because of the high energetic cost of translation. Low carbon conversion factors within subseafloor anaerobic feeding chains account for exponential declines in cellular biomass in the fermentation zone of anoxic sediments. Our analysis points to the existence of a life–death transition zone in which the last biologically catalyzed life processes are replaced with purely chemical reactions no longer coupled to life.

Keywords: deep biosphere; fermentation; syntrophy; methanogenesis; limits to life; anaerobic physiology

There is a great deal of interest in microbial processes in anaerobic sediments. Most of the Earth's surface is covered by sediment, and the amount of biomass sequestered there rivals the amount of biomass in the oceans above it. It is known that in the transition zone from methanogenesis to sulfate reduction (Fig. 1), methane from methanogenesis disappears. Below this depth, in the deeper anoxic sediments, the feeding chain starts with fermentation and is short (Parkes, Cragg and Wellsbury 2000). Most of the available organic matter in deep sediments is microbial necromass (Lomstein *et al.* 2012), and most of the
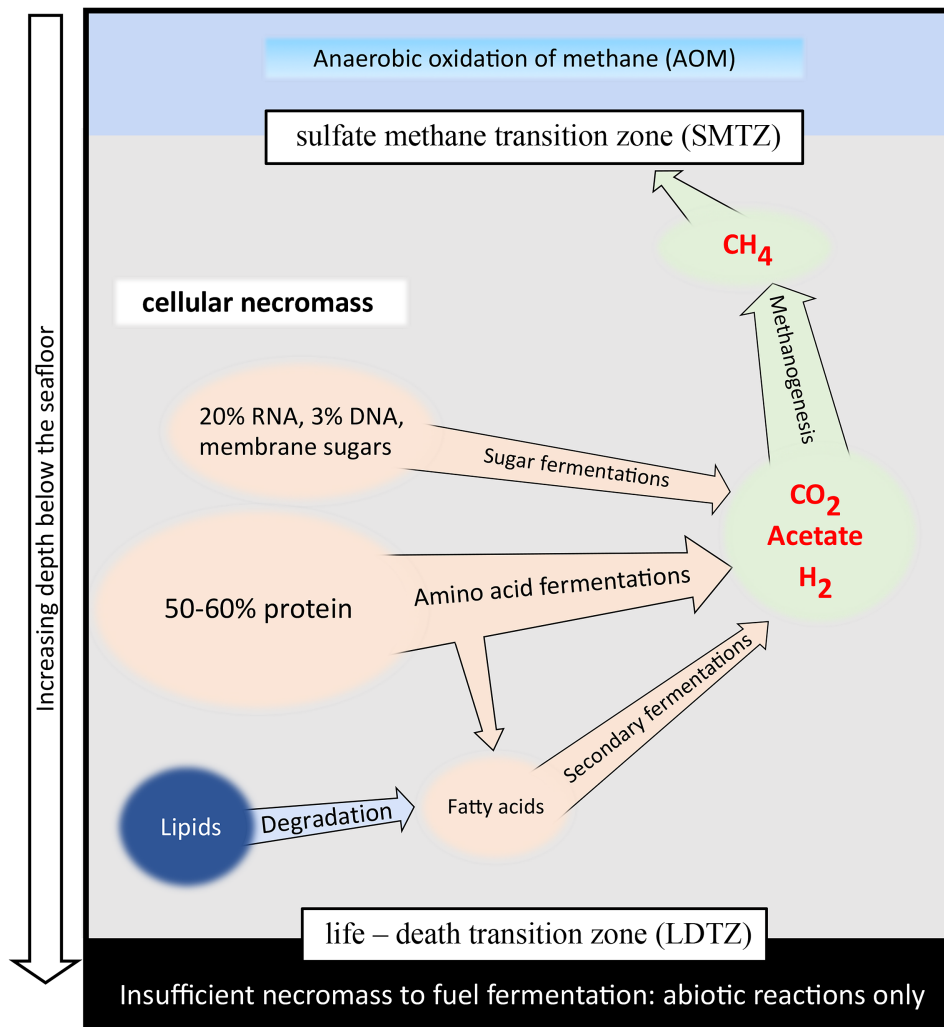
Figure 1. Physiological considerations of cell mass conversions in anoxic subseafloor sediment. Most of the fermentable substrates are amino acids from dead cells, and the resulting fermentation products result in an upper boundary limit for mass carbon conversion to methanogens of 100:1 (from acetate). Lipids are not fermentable, but degradation products such as fatty acids can be fermented in syntrophic secondary fermentations. Fermentable substrates are shown in pink colors. SMTZ: sulfate methane transition zone.

fermentable necromass is in the form of proteins and amino acids because cells are mostly protein by weight.

Oxidants such as Fe[III], Mn[IV], SO_4^{2-} or NO_3^- that could serve as terminal acceptors for microbes to drive the oxidation of reduced carbon compounds are generally thought to be depleted below the sulfate methane transition zone (SMTZ; Bowles *et al.* 2014). In anoxic marine sediments, these oxidants are typically used up (reduced) closer to the seafloor surface, whereas deep below the SMTZ in the subseafloor, they are lacking because these settings are insulated from nutrient exchange with ocean water or hydrothermal systems (Parkes, Cragg and Wellsbury 2000). In such systems, extreme energy limitation is thought to play a major role (Hoehler and Jørgensen 2013; Lever *et al.* 2015), and fermentations are dominant (Bowles *et al.* 2014) that require organic compounds of intermediate oxidation states as terminal acceptors.

In subseafloor sediment, there exists a global trend of exponentially decreasing cell densities with depth (Kallmeyer *et al.* 2012). There are some exceptions at redox transition zones (D'Hondt *et al.* 2004; Parkes *et al.* 2005), but below these zones—in the fermentation zone—the trend of net death continues. The question 'why are the cells always dying faster than they are growing?' concerns the fate of individual cells and their individual adenosine triphosphate (ATP) budgets. Thus, an

understanding of the bioenergetic stoichiometry of the relevant necromass fermentations would help to set boundary conditions for production of new cell biomass based on carbon and energy availability. To our knowledge, energetic boundary conditions have not been constrained with ATP consumption and production budgets of relevant fermentation-based metabolisms.

Here, we consider the energetic stoichiometry of the anoxic subseafloor fermentation zone where amino acids are quantitatively the most important substrate for fermentation reactions (Lever *et al.* 2015), the end products of which support methanogens in proximity to the transition zone of anaerobic sediments where methane disappears (Parkes, Cragg and Wellsbury 2000). Our analysis constrains the energetic boundary conditions of this net-death ecosystem with ATP consumption and production budgets of relevant fermentation metabolisms, to obtain an order of magnitude estimate on an upper limit to how much growth in anoxic sediment can result from fermented microbial necromass. The calculations show that amino acid fermentation reactions all yield maximum ATP levels insufficient to result in a net increase in cellular biomass, given the high energetic cost of protein biosynthesis. Our analysis shows that below the SMTZs where fermentation and methanogenesis dominate, fermentation of necromass simply does not provide enough energy to support net growth. Rather, our calculations

imply an exponential drop-off in cell biomass over time as has been observed on a global scale (Kallmeyer *et al.* 2012) in deep anoxic subseafloor sediment.

THE FERMENTATION ZONE

Sediment moves upward with new incoming sediment at the surface. Fermentations occur throughout marine sediment. Our focus in this paper concerns processes in the fermentation zone that begins below the SMTZ. We furthermore focus on isolated sediment that does not receive an influx of nutrients or electron acceptors such as sulfate, Fe oxides or Mn(IV). The fermentation zone below the SMTZ is dominated by fermenters and methanogens. Fermenters live by degrading the cell mass that the overlying aerobes, nitrate respirers and sulfate reducers left behind. Fermentations produce mainly H_2, CO_2 and acetate that fuel the methanogens, which produce methane that in turn fuels anaerobic methane oxidation at the overlying SMTZ (Fig. 1). Most of the available organic matter in deep sediments is microbial necromass (Lomstein *et al.* 2012; Braun *et al.* 2017). Most of that necromass is in turn protein, because cells are ∼50% protein by dry weight.

Fermentations do not require a supply of external terminal acceptors; they are disproportionation reactions of organic compounds having an intermediate oxidation state. Fermentations support ATP synthesis by substrate level phosphorylation or chemiosmotic coupling (Buckel and Thauer 2013). Lipids and fatty acids are too reduced for simple fermentations; they need to be degraded by syntrophic associations of fermenting bacteria with methanogenic partners (Fig. 1). In contrast, amino acids, nucleic acid bases and sugars are easily fermentable substrates (Barker *et al.* 1961; Barker 1981; Brasen *et al.* 2014).

In the fermentation zone (below the SMTZ), cell mass is the main substrate for fermenters (Lever *et al.* 2015). By weight, exponentially growing cells are made of roughly 50–60% protein, 20% RNA, 10% lipids, 3% DNA, ∼10% sugars as cell wall constituents and some metabolites (Stouthamer 1973; Neidhardt, Ingraham and Schaecter 1990; Lengeler, Drews and Schegel 1999). Well-fed cells can contain considerable amounts of glycogen, >10% by weight. Cells in sediments are generally regarded as starved (Hoehler and Jørgensen 2013) and for our purposes can be regarded as having little, if any, glycogen content. Because lipids are degraded relatively slowly (Xie *et al.* 2013), protein, RNA and to a lesser extent DNA, remain as the main substrates. There are also viruses in the fermentation zone (Orsi 2018). They are about two orders of magnitude smaller than cells, but there are about two orders of magnitude more of them (Engelhardt *et al.* 2014) such that they represent a quantitatively similar amount of protein and nucleic acid substrate for fermentations as the cell populations from which they stem. It is well known that starved cells are much smaller than exponentially growing cells (Lever *et al.* 2015), but we will be looking at the issue of how many starving cells can arise from the fermentation products of other starving cells; so, if all cells are small, our conversions should not be heavily affected.

The energetically most demanding task that a cell does during growth is protein synthesis (Stouthamer 1979), which requires ∼75% of the cell's energy budget, with ribosomes constituting ∼40% of the cell by weight. In energy-limited environments like sediments, maintenance and survival are more important than growth (Hoehler and Jørgensen 2013). Cryptic elemental cycles occur in the fermentation zone such as sulfate reduction (Holmkvist, Ferdelman and Jørgensen 2011), but these are predicted to result in limited amounts of activity (Hoehler and Jørgensen 2013). Fermentations are thus the major source of

energy below the SMTZ; so, it is worthwhile to obtain an order of magnitude estimate that might put an upper limit to how much growth in the anaerobic sediment column can result from how much fermented biomass.

FERMENTATION PRODUCTS

While the substrate for fermentations (cell mass) is straightforward, the fermentations themselves are not (LaRowe and Amend 2019). Most of the cellular mass is in the form of protein, and the main organic substrates available for living cells in the subseafloor fermentation zone are other dead cells (Lomstein *et al.* 2012). Amino acids are thus the main fermentable substrates. Typical products of bacterial amino acid fermentations are CO_2, NH_4^+, acetate, butyrate and some H_2 (Smith and Macfarlane 1997).

Amino acid fermentations entail ATP synthesis by substrate level phosphorylation (SLP) and by ion gradient phosphorylation using chemiosmotic coupling and ATPases at the cytoplasmic membrane. In fermenters studied in detail so far, the quantitative contributions of SLP and ion gradients to ATP synthesis are roughly equal and are often interconnected by flavin-based electron bifurcation (Buckel and Thauer 2013). Flavin-based electron bifurcation is a mechanism of energy coupling in anaerobes that interconverts ferredoxin pools, reduced nicotinamide adenine dinucleotide (NADH) pools and, in cooperation with Rnf complexes (Na^+/H^+-pumping NAD ferredoxin reductases), ion gradients at the plasma membrane (Müller, Chowdhury and Basen 2018). Although bifurcation is central to energy conservation in many strict anaerobes, it was discovered only recently (Herrmann *et al.* 2008); hence, complete maps with full stoichiometry, redox and energy balance are available for only a few well-studied fermentation systems.

Well-studied examples of amino acid fermentations are pathways of glutamate fermentation. There are five different pathways of glutamate fermentation (Buckel 2001; Plugge *et al.* 2001). Two of the pathways of glutamate fermentation that have been studied in detail, one from *Clostridium tetanomorphum* and one from *Acidaminococcus fermentans*, produce exactly the same end products in exactly the same amounts with exactly the same energy yields, but entail different chemical intermediates in the fermentation process and unrelated enzymes (Buckel and Barker 1974). The overall reaction is

$$5 \text{ glutamate}^- + 2\,H_2O + 2H^+ \rightarrow 5\,NH_4^+ + 5\,CO_2 + H_2$$
$$+ 6 \text{ acetate}^- + 2 \text{ butyrate}^-,$$
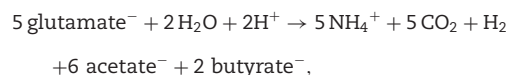
with an energy yield of 0.95 ATP per glutamate and a free energy change of $\Delta G_o{'} = -63$ kJ per mol glutamate (Buckel and Thauer 2013). Per 5 glutamate, the pathway generates 3 ATP by SLP and 3 ATP by a Na^+-dependent ATPase, but one pumped Na^+ is expended for each glutamate imported, hence the non-integer ATP yield (Buckel and Thauer 2013). The soluble enzymes involved in the two pathways are different, the reactions harnessed for pumping are also different and electron bifurcation is centrally involved in the pathway of both fermenters (Buckel and Thauer 2013). A similar situation is encountered for glucose fermentations in *Thermotoga maritima* and *Pyrococcus furiosus*, the pathways and enzymes are different and the overall reactions are the same

$$\text{glucose} + 2\,H_2O \rightarrow 2 \text{ acetate}^- + 2\,H^+ + 2\,CO_2 + 4\,H_2,$$

with an energy conservation of 2–4 ATP per glucose, 1.5 ATP generated by SLP and 1.5 generated by chemiosmotic coupling. At low temperature and low hydrogen pressure, up to 4 ATP can be synthesized (Müller *et al.* 2008).

In terms of sediment fermentation processes, protein and nucleic acids are, by weight, the main substrates; so, we focus on them here. Proteins are broken down extracellularly by proteases; peptides are imported and hydrolyzed to amino acids. In bacteria, amino acids can be fermented by reactions similar to the case of glutamate fermentation above, or by Stickland reactions (Barker *et al.* 1961), in which one amino acid is oxidized while another one is reduced. *Clostridium sticklandii* is a bacterial generalist amino acid fermenter that can metabolize all amino acids in Stickland reactions except Ala and Glu (Fonknechten *et al.* 2010). A key enzyme of Stickland reactions is glycine reductase (Andreesen 2004), a selenoprotein that generates acetyl phosphate for SLP from glycine reduction. However, no glycine reductase was found to be expressed in subseafloor metatranscriptomes (Orsi *et al.* 2013) suggesting that alternative mechanisms of amino acid fermentation might takeplace.

In Archaea, amino acid fermentations (Adams and Kelly 1994) typically involve conversion of the amino acids to the corresponding 2-oxoacids by transaminases; the 2-oxoacids are oxidatively shortened by 2-oxoacid oxidoreductases that generate CO_2, reduced ferredoxin and acyl-CoA. Ferredoxin is typically reoxidized by hydrogenases; acyl-CoA typically yields acyl-phosphate as an intermediate and ATP by substrate level phosphorylation, releasing the corresponding short-chain fatty acid, or volatile fatty acid (VFA). This is evidenced in the accumulation of VFAs in the fermentation zone of anoxic sediments (D'Hondt *et al.* 2003), and by newly discovered yet uncultivated Archaea living in the fermentation zone of anoxic marine sediment featuring an amino acid fermentation-based metabolism (Lloyd *et al.* 2013). Furthermore, two novel Archaea that were obtained and imaged in enrichment cultures from marine sediment were both amino acid fermenters, 'Korarchaeaon cryptophilum' (Elkins *et al.* 2008) and 'Prometheoarchaeum syntrophicum' (Imachi *et al.* 2020). Peptide-fermenting Archaea such as *Pyrococcus furiosus* can possess as many as 10 different 2-oxoacid oxidoreductases that will accept as substrates the 2-oxoacids stemming from deamination of Ala, Thr, Cys, Met, Val, Leu, Ile, Phe, Tyr, Trp, His, Arg, Glu and Gln (Scott, Poole and Adams 2014).

In order to maintain redox balance, electrons generated from oxidative steps of amino acid fermentation (deaminations and decarboxylations) have to be excreted, typically in the form of reduced molecules such as H_2, formate (Zindel *et al.* 1988) or as aliphatic residues in organic acids such as acetate or butyrate. This can involve a variety of reactions including Stickland reactions (Andreesen 2004), reduction of crotonyl-CoA (Buckel and Thauer 2013), reduction of protons using soluble hydrogenases as in *Thermotoga* (Schut and Adams 2009) or membrane-bound hydrogenases as in *Pyrococcus* (Yu *et al.* 2018). Below the STMZ in deep anaerobic sediment, CO_2 and H_2 can be used by methanogens for ATP synthesis and carbon assimilation, whereas the other end products of amino acid fermentation, namely acetate, short chain fatty acids and NH_4^+ accumulate transiently in the environment (D'Hondt *et al.* 2004).

GROWTH FROM FERMENTATION PRODUCTS

Through the archaeal or the bacterial fermentation pathways, each amino acid generates approximately one ATP, one acetate, two H_2 (including some H_2 hidden in butyrate), one CO_2 and one NH_4^+. We have neglected the cost of peptide import, which if

it lies in the range of one ATP per deca- to pentapeptide via an ABC-type peptide importer would consume 10–20% of the ATP budget; *Acidaminococcus fermentans,* for example, requires 0.25 ATP (one Na^+) per imported glutamate (Buckel and Thauer 2013). For estimating methanogenesis in the next section, we generously estimate that fermentations can provide two H_2, CO_2 and acetate each per amino acid, in addition to one ATP and one NH_4^+, plus substoichiometric amounts of other organic acids.

Nucleic acids can also be fermented. Actively growing cells contain ~20% RNA by weight (Stouthamer 1973; Neidhardt, Ingraham and Schaecter 1990; Lengeler, Drews and Schegel 1999), though this might be somewhat lower in the ultraslow growth state of the deep biosphere (Hoehler and Jørgensen 2013). Known pathways of purine fermentation can yield one ATP per purine (Barker *et al.* 1961), and some cells that can satisfy their carbon and energy needs from purines alone (Hartwich, Poehlein and Daniel 2012). It should furthermore be possible to obtain one ATP per pyrimidine as well using known pathways (Schönheit *et al.* 2016). That leaves ribose. RNA is ~40% ribose by weight; cells are 20% RNA, hence ~8% ribose by weight. Ribose is probably the most abundant pure sugar in deep sediment. It can enter catabolic pathways by a number of routes (Brasen *et al.* 2014). A novel pathway is the ribose bisphosphate pathway that seems to be present in subsurface microbial fermenters (Wrighton *et al.* 2012). This pathway involves the once puzzling ribulose-1,5-bisphosphate carboxylase that was found in the genome sequence of many heterotrophic archaea (Aono *et al.* 2015). RNases degrade RNA to ribonucleoside 5′-monophosphates, a phosphorylase cleaves the base, which can be degraded to yield one ATP, from the ribose backbone. This yields ribose-1,5-bisphosphate, which is converted by an isomerase to ribulose-1,5-bisphosphate, the substrate for RuBisCO (Aono *et al.* 2015), which carboxylates the substrate to yield two molecules of 3-phospho-D-glycerate (3PGA). 3PGA is an intermediate of glycolysis that can yield one ATP at the pyruvate kinase reaction and one more ATP from pyruvate oxidation via the 2-oxoacid oxidoreductase, yielding CO_2, H_2 and acetate as above. That yields four ATP per ribose, about one each per base or about five ATP per nucleoside; we subtract one ATP per rNMP for import, yielding about four ATP plus two H_2, two acetate and one CO_2 per base.

Homoacetogenesis combines the fermentation of sugars with H_2-dependent CO_2 reduction by acetogenic microbes and may also be a key form of metabolism in deep anoxic subseafloor sediment (Lever *et al.* 2009; Lever 2012; He *et al.* 2016; Martin *et al.* 2016; Sewell, Kaster and Spormann 2017). Indeed, homoacetogenic fermentation of glucose has the highest ATP yield of any sugar fermentation reaction yet studied, 4.3 ATP/mol glucose fermented (Müller 2008). The widespread nature of homoacetogenic metabolism in Chloroflexi (Kaster *et al.* 2014; Sewell, Kaster and Spormann 2017), 'Atribacteria' (Nobu *et al.* 2016; Katayama *et al.* 2019) and Archaea (He *et al.* 2016; Martin *et al.* 2016; Orsi *et al.* 2019) that are ubiquitous in subseafloor anoxic sediments indicates that homoacetogenesis is a common form of fermentation in these settings. Most likely, because it is a relatively energy efficient anaerobic metabolism (Schuchmann and Müller 2016), it is apparently selected for under these extremely energy limited conditions (Orsi *et al.* 2019). Remarkably, one of the most ubiquitous groups in anoxic subseafloor sediments, the candidate Phylum 'Atribacteria' (Orsi 2018), was recently isolated in pure culture and was found to have a hydrogenogenic fermentative metabolism (Katayama *et al.* 2019) confirming earlier metagenomic predictions (Nobu *et al.* 2016).

SYNTROPHY AND SECONDARY FERMENTATIONS

Three observations indicate that amino acid fermentations are ongoing in deep sediment. Amino acid concentrations decrease from micromolar concentrations at the sediment surface down to nanomolar concentrations in the fermentation zone in sediments with ages over one million years old (Braun *et al.* 2017). Genes involved in amino acid metabolism have been found in multiple anoxic subseafloor settings to have a relatively high expression level in the fermentation zone (Orsi *et al.* 2013; Bird *et al.* 2019). Ammonium (D'Hondt *et al.* 2004), short chain fatty acids (D'Hondt *et al.* 2003) and the amino acid fermentation product γ-amino butyric acid (Møller *et al.* 2018) accumulate in the fermentation zone of anoxic sediments. Under anoxic conditions, fatty acids are degraded by syntrophic associations of fermenting bacteria with methanogenic partners (Fig. 1; Schink 1997). Syntrophy is important for survival in deep anoxic subseafloor sediment (Parkes, Cragg and Wellsbury 2000), because it links fermentation to methane production (Schink 1997).

Most syntrophic reactions are secondary fermentations in which organisms ferment the fermentation products of other anaerobes. Amino acid fermentations yield butyrate:acetate ratios of roughly 1:3 (Schink 1997). The concentration of butyrate is 100 times lower than acetate in anoxic subseafloor sediments (Glombitza *et al.* 2019), indicating microbial consumption of butyrate via secondary fermentation reactions. Butyrate can be consumed via secondary fermentation, producing acetate and H_2, and providing $\sim$0.3 ATP per butyrate fermented (Schink 1997).

$$Butyrate^- + 2\,H_2O \rightarrow 2\,CH_3COO^- + H^+ + 2\,H_2$$
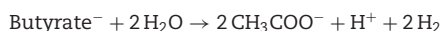
This reaction is energetically favorable only in the presence of a H_2-consuming syntrophic partner, e.g. a methanogen (Schink 1997). The low concentrations of butyrate relative to acetate (Glombitza *et al.* 2019) thus suggest that active syntrophic consortia of butyrate fermenting cells and H_2-oxidizing partner cells exist in the fermentation zone of deep anoxic sediments. In a similar manner, long-chain fatty acids from lipid degradation are fermented to acetate and H_2 in the presence of H_2-oxidizing partners. The short-chain fatty acids butyrate (C4), caproate (C6) and caprylate (C8) can furthermore be produced from exergonic 'chain elongation' reactions involving ethanol and acetate, which yields $\sim$1 ATP in *Clostridium kluyveri* (Angenent *et al.* 2016). A recent study (Glombitza *et al.* 2019) analyzing volatile fatty acids in anoxic subseafloor sediment showed that there is an order of magnitude more propionate compared to butyrate, and thus we also considered production and consumption of propionate. Propionate is produced under anoxic conditions—among others—via lactate fermentation (Lens, Dijkema and Stams 1998), and the resulting propionyl-CoA is used to convert lactate to lactyl-CoA, which is dehydrated to acrylyl-CoA and reduced to propionyl-CoA (Buckel and Thauer 2018) such that no ATP is generated.

THERMODYNAMICS AT LOW SUBSTRATE CONCENTRATIONS

We used thermodynamics to predict the favorability of certain fermentation reactions in anoxic sediments. The standard term $\Delta G^{\circ\prime}$ is defined as the enthalpy of a reaction under standard conditions: all reactants = 1.0 M, except $[H_2O]$ = 55.6 M, pH = 7.0;

[gases] = 100 kPa (1 atm); and T = 298 K. The $\Delta G^{\circ\prime}$ values are calculated from the ΔG°_f values of the formation of the reaction partners from the elements (Thauer, Jungermann and Decker 1977; Buckel and Miller 1987). $\Delta G'$ is defined as the enthalpy of a reaction under any condition using the following equation:

$$\Delta G' = \Delta G^{\circ\prime} + RT \ln \Pi\,[\text{Products}] \times \Pi[\text{Substrates}]^{-1} = \Delta G^{\circ\prime}$$
$$+5.7 \log \Pi\,[\text{Products}] \times \Pi[\text{Substrates}]^{-1} \text{kJ/mol at } 298^{\circ}\text{K}$$

The expected maximum ATP yield in a fermentation, either by SLP (substrate level phosphorylation) or ETP (electron transport phosphorylation) can be calculated as $\Delta G'/(-76\text{ kJ/mol})$ (Thauer, Jungermann and Decker 1977). For example, oxidation of glucose ($C_6H_{12}O_6$) with 6 O_2 to 6 CO_2 + 6 H_2O ($\Delta G^{\circ\prime}$ = -2870 kJ/mol) in a cell with mitochondria yields up to 38 ATP. Hence, $-2870/38 = -76$ kJ/mol from the fermentation is the minimum requirement for the synthesis of 1 mol ATP. For more than four decades, this value has provided a good estimate of ATP yield in most fermentations, especially since it has become evident that anaerobes conserve energy via not only substrate phosphorylation but also electron transport (ion gradient) phosphorylation. Under standard equilibrium conditions, however, hydrolysis of ATP to P_i and ADP yields $\Delta G^{\circ\prime} = -32$ kJ/mol. But in a cell, at 1 mM concentrations, the free energy falls to $\Delta G' = \Delta G^{\circ\prime} + 5.7 \log [ADP] \times [P_i] \times [ATP]^{-1} = -32 + 5.7 \times (-3) = -49$ kJ/mol. The remaining $-76 - (-49) = -27$ kJ/mol is due to irreversible heat-releasing processes that occur in all fermentations.

In pore waters of anoxic freshwater lake sediments, we find fatty acids and acetate at concentrations of few micromolar, and H_2 at 10 to 1 Pa (Montag and Schink 2018). These concentrations find their lower limits in the range of $\sim$10 μM and 1 Pa because only above these thresholds will their conversion to methane yield sufficient energy to keep the respective methanogens running (Schink 1997). In marine sediments, H_2 concentrations are lower in the nM to μM range, and correlate positively with organic matter concentrations (Lin *et al.* 2012). On the other hand, concentrations of amino acids and sugars in deep sediments can vary widely from site to site and are somewhere in the nanomolar to micromolar ranges but generally decrease in concentration with depth below the seafloor (Burdige 2002, 2006; Lomstein *et al.* 2012). Thus, exact calculations of energy yields of fermenting bacteria that capture the full range of *in situ* substrate concentrations are difficult, but one can estimate ranges.

In Table 1, we examined the changes in free energy, designated as $\Delta G'^1$ where the concentrations of all reactants are 1000 times lower (1 mM, gases at 100 Pa = 10^{-3} atm) and $\Delta G'*$ at the more realistic concentrations (10 μM, gases at 10 Pa). We used previously studied fermentation reactions for glutamate (Buckel and Thauer 2013), alanine (Buckel and Thauer 2018), glucose (Buckel and Thauer 2013) and lactate (Buckel and Thauer 2018) in order to calculate the $\Delta G'^1$ and $\Delta G'*$ values, all of which result in a more favorable free energy and higher net ATP yield compared to $\Delta G^{\circ\prime}$ (Table 1). The increased efficiency at lower concentrations is due to a smaller number of substrates compared to products (5 glutamates give 19 products). Any fermentation processes producing more product molecules than consuming substrate molecules will become more exergonic at lower concentrations of the reaction partners (Le Châtelier's principle; Thauer, Jungermann and Decker 1977). Moreover, already at 1 mM glutamate, a much simpler pathway of glutamate fermentation could be possible where direct production of hydrogen from reduced ferredoxin, formed by pyruvate-ferredoxin oxidoreductase, could be coupled to ATP synthesis, resulting in $\sim$1

Table 1. Free energies and estimated net ATP yields from fermentation reactions at different substrate and product concentrations except for hydrogen as indicated, 55 M water and pH 7.0. The equations in bold letters below the table are experimentally established reactions, whereas the others, which produce more hydrogen, most likely are used at concentrations around 1 mM and lower. The ranges of amino acid and sugar substrate concentrations cover those measured in marine sediments (Burdige 2002), which can vary widely from site to site but generally decrease in concentrations with increasing depth below the seafloor (Burdige 2006; Lomstein *et al.* 2012). Concentrations of H_2 in anoxic sediments also vary from nM to μM concentrations but tend to co-vary with concentrations of organic matter that are the source of H_2 from fermentations (Lin *et al.* 2012). The mechanistically calculated ATP yields are given as mol ATP/mol substrate. A "cannot proceed" means that the reaction cannot proceed as indicated. At lower substrate/product concentrations, the ATP yield is probably the same as that at the higher concentration. Alanine and lactate are fermented either via acrylyl-CoA or via methylmalonyl-CoA, which yield 0.33 or 0.67 ATP/alanine and lactate, respectively (Buckel and Thauer 2018). The maximum ATP/substrate yield can be calculated from $\Delta G^{\circ\prime}$/substrate divided by -76.

Reaction	1 M substrate 100 kPa H_2		1 mM substrate 100 Pa H_2		10 μM substrate 10 Pa H_2	
	$\Delta G^{\circ\prime}$/reaction	ATP/substrate	$\Delta G^{\prime 1}$/reaction	ATP/substrate	$\Delta G^{\prime}*$/reaction	ATP/substrate
Glutamate 1	-319 kJ	0.9	-547 kJ	cannot proceed	-712 kJ	cannot proceed
Glutamate 2	-43 kJ	cannot proceed	-111 kJ	1.0	-151 kJ	1.0
Alanine 1	-162 kJ	0.3–0.7	-230 kJ	cannot proceed	-299 kJ	cannot proceed
Alanine 2	-143 kJ	0.7	-280 kJ	0.3–0.7	-411 kJ	0.3–0.7
Lactate 1	-168 kJ	$0.3-0.7$	-185 kJ	0.3–0.7	-197 kJ	cannot proceed
Lactate 2	-98 kJ	cannot proceed	-184 kJ	0.3–0.7	-223 kJ	0.3–0.7
Glucose	-216 kJ	cannot proceed	-353 kJ	4.0	-450 kJ	4.0
Pyruvate	-52 kJ	cannot proceed	-86 kJ	1.0	-103 kJ	1.0

Glutamate 1: 5 Glutamate$^-$ + 6 H_2O + 2 H^+ $\rightarrow$ 5 NH_4^+ + 5 CO_2 + H_2 + 6 Acetate$^-$ + 2 Butyrate$^-$

Glutamate 2: Glutamate$^-$ + 2 H_2O $\rightarrow$ NH_4^+ + CO_2 + H_2 + 2 Acetate$^-$

Alanine 1: 3 Alanine + 2 H_2O $\rightarrow$ 3 NH_4^+ + CO_2 + Acetate$^-$ + 2 Propionate$^-$

Alanine 2: 3 Alanine + 4 H_2O $\rightarrow$ 3 NH_4^+ + 2 CO_2 + 2 Acetate$^-$ + Propionate$^-$ + 2 H_2

Lactate 1: 3 Lactate$^-$ $\rightarrow$ CO_2 + Acetate$^-$ + 2 Propionate$^-$ + H_2O

Lactate 2: 3 Lactate$^-$ + H_2O $\rightarrow$ 2 CO_2 + 2 Acetate$^-$ + Propionate$^-$ + 2 H_2

Glucose: Glucose + 2 H_2O $\rightarrow$ 2 CO_2 + 2 Acetate$^-$ + 2 H^+ + 4 H_2

Pyruvate: Pyruvate$^-$ + H_2O $\rightarrow$ CO_2 + Acetate$^-$ + H_2

ATP/glutamate (Table 1). In this much simpler pathway, electron bifurcation and energy conservation via $\Delta\mu Na^+$ (generated by Rnf, a ferredoxin:NAD reductase) would not be required. In addition, the production of ammonia helps to drive the reaction forward, because fermentations of carbohydrates such as lactate yield water instead. This additional push, however, comes to effect only at very low concentrations. The fermentations with higher H_2 production reveal smaller efficiencies under standard conditions ($\Delta G^{\circ\prime}$) but increase at lower concentrations (Table 1).

LIVING FROM FERMENTATION LEFTOVERS

For the constituents of dead cells to generate a live cell, if we look just at the main components, it is advisable to recycle amino acid residues after partial degradation, i.e. deamination and decarboxylation, as this was shown for anaerobic microbial communities in rumen contents (Allison and Bryant 1963). Complete degradation of amino acids yields ~2 ATP per amino acid at best, but to make a new cell that contains the same amount of protein we need to expend 4 ATP per peptide bond at translation, plus occasional error correction or ~5 ATP per amino acid polymerized. Five amino acids need to be consumed to make one new peptide bond (an additional, 6th amino acid), such that even if we import amino acids for <0.25 ATP per amino acid, from the amino acid standpoint alone, one generation of cells gives rise to roughly 1/6 (maximally 1/3) the number of progeny on a per-weight basis, no maintenance energy, protein unfolding or uncoupling considered. In terms of what is possible converting one cell to (what fraction of) another, the curve falls quickly, much more steeply than 1/6, 1/36, 1/216 in deep anoxic sediment settings where the resources are finite and consumed. This steep downward trend toward chemical equilibrium (what life tries to avoid) is exactly what Finkel (2006) found for starving cells, albeit in the presence of oxygen. We arrive at the same general conclu-

sion from stoichiometric conversion rates of the main substance of cells (amino acids) for making protein out of protein in heterotrophic survival, that is, without coupling it to ATP formation in methanogens.

The carbon conversion ratio for RNA is similarly low, because ribonucleoside monophosphates need to be activated (2 ATP) for polymerization, in addition to processing and post-transcriptional modifications that need to be performed, and every monomer incorporated is one that the cell cannot use for energy conservation. Starved cells are much smaller than exponentially growing ones, indicating simply that staying alive as opposed to growing is a successful strategy in low-energy environments (Lever *et al.* 2015).

What about the H_2, CO_2 and acetate that arise from fermentation? How much methanogenesis can they support? Each amino acid in the dead cell has on average five carbon atoms and generates one CO_2 in fermentation. Methanogens, unless they supply themselves with partly degraded amino acids from fermenting bacteria (Allison and Bryant 1963), generate their amino acids from acetate and CO_2. The growth yield of 1.6 g of cells (dry weight) per mol of CH_4 produced as reported for *Methanobacterium thermoautotrophicum*, a methanogen that lacks cytochromes, grown on H_2 and CO_2 (Schönheit, Moll and Thauer 1980) delivers an estimate of one molecule of carbon being fixed for every 18.5 molecules of CH_4 produced. Rounding that corresponds to ~20 molecules of CO_2 that go through the cell to be reduced to methane for every CO_2 that is incorporated into cell mass. For acetogens (Daniel *et al.* 1991) the reported ratio is 24:1. For a methanogen growing on H_2 and CO_2, ~21 fermented amino acids (20 CO_2) are required to supply one CO_2 for methanogen cell mass; ~100 fermented amino acids are required to make one average methanogen amino acid with 5 carbons (Fig. 2). Nitrogen is not limiting, as NH_4^+ is abundant in deep anoxic sediment (D'Hondt *et al.* 2004). Those 100 fermented amino acids deliver
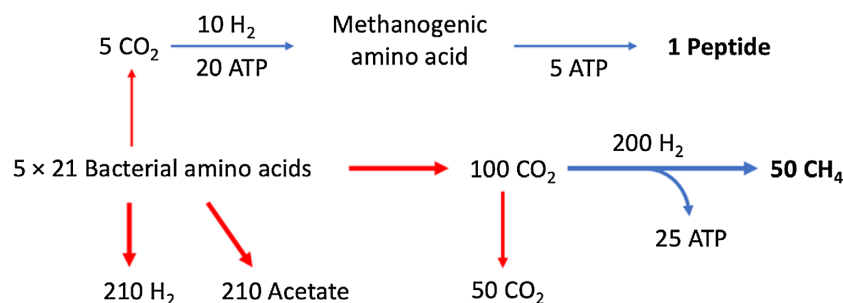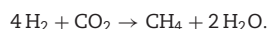
Figure 2. Fermentation of 105 bacterial amino acids (C5) to synthesize one peptide unit (C5) in a methanogenic archaeon. Red lines: fermentations, blue lines: methanogenic activities.

100 H$_2$, which is the amount required to make only 25 methane (Fig. 2) according to the methanogenic reaction

$$4\,H_2 + CO_2 \rightarrow CH_4 + 2\,H_2O.$$

Starting from H$_2$ and CO$_2$, in order to make 100 methane to support the synthesis of one average methanogen amino acid, a fermenting community has to disproportionate 200 amino acids (without H$_2$ loss to the environment). Add to that the ATP that is required to make a peptide bond. We can estimate a methanogen requirement of 5 ATP per peptide bond, four at translation plus one for nutrient import, misincorporation, misfolding and the like (Fig. 2). ATP is provided by methanogenesis at 0.5 ATP per CH$_4$ (Thauer *et al.* 2008); 5 ATP require 10 CH$_4$ which in turn requires 40 H$_2$ or 20 amino acids if each amino acid supplies two H$_2$, partly through secondary fermentations.

Thus, for a methanogen growing on H$_2$ and CO$_2$ and synthesizing all amino acids from CO$_2$, fermenters would need to disproportionate 220 amino acids. For an idealized methanogen growing on H$_2$ and CO$_2$ and synthesizing no amino acids at all, importing and assimilating all amino acids from the environment while obtaining ATP from methanogenesis, fermenters would need to disproportionate 20 amino acids for each methanogen peptide bond (Fig. 2), but they would also need to leave a substantial proportion of their growth substrate (amino acids) untapped to enable methanogen amino acid assimilation. These values (∼200:1 and ∼20:1) probably represent upper and lower bounds on carbon conversion rates for conversion of fermented cell mass into methanogen protein, the main component of cell mass, in sediment where no other nutrients such as sulfate or nitrate enter the system. Just looking at protein, which is likely to be the limiting factor for survival, the conversion of C from fermented dead cell protein into C of methanogen protein via H$_2$ and CO$_2$ occurs at a ratio of ∼200:1 in terms of net *de novo* protein synthesis ('growth', which is not the norm for energy-limited environments) if growth is supported by diffusing gasses (H$_2$ and CO$_2$) or ∼20:1 if methanogens are efficiently competing with fermenters for amino acids.

If methanogenesis is being fueled by acetate instead of H$_2$ and CO$_2$, and if we assume that the fermenters are generating two H$_2$, CO$_2$ and acetate per degraded amino acid, the picture is less bleak by about a factor of 2. That is because methanogenesis from acetate (aceticlastic methanogenesis) converts acetate to methane

$$CH_3COO^- + H^+ \rightarrow CH_4 + CO_2,$$

yielding ∼0.3 ATP per acetate consumed (Schlegel *et al.* 2012; Welte and Deppenmeier 2014). The growth yields (grams of cells

per methane) for methanogens growing on acetate are in the range of 1.5–3 g per mol methane produced (Welte and Deppenmeier 2014), similar to those for growth on H$_2$ and CO$_2$ (Thauer *et al.* 2008). Evidence exists that in deep subseafloor fermentation zones, some acetate carbon may be mineralized first to CO$_2$, prior to being reduced to methane with H$_2$ (Beulig *et al.* 2018).

Methanosarcina species have a lower affinity for acetate in the environment because they use a different system of acetate activation involving acetate kinase, which has a ∼100-fold higher K$_m$ for acetate than the acetyl-CoA synthase (AMP-forming) used by *Methanosaeta* species (Welte and Deppenmeier 2014). The consequence is that *Methanosarcina* species require ∼1 mM acetate for growth, whereas *Methanosaeta* species can survive with 7–70 µM acetate (Welte and Deppenmeier 2014). That might be relevant in deep sediment, where acetate levels have been measured at the low micromolar range (D'Hondt *et al.* 2003). However, acetate activation in *Methanosaeta* species is energetically more costly, so that the growth yield is lower, on the order of 1.5 g per mol of acetate consumed. The similar growth yields per methane from acetate vs H$_2$ and CO$_2$ mean that also for growth on acetate, about one CO$_2$ is fixed as cell mass per 20 methane produced. Instead of two fermented amino acids to make 4 H$_2$, one acetate generates one methane, so that ∼100 amino acids (rather than 200) would need to be fermented to make one new methanogen amino acid. We generously assume growth yields similar to those for exponentially growing cells in lab cultures and no product losses, such that these carbon conversion rates represent best-case scenarios.

Our calculations indicate that cell division is probably not the primary mode of substrate turnover. Replacing old proteins with new ones within the same cell (reusing one's own amino acids) is a far more likely fate for amino acids within the methanogens, because the average sized 5-carbon amino acids are already within the cell. Such processes of replacing old or damaged proteins might constitute a good portion of maintenance, a still poorly understood component of long-term survival (Hoehler and Jørgensen 2013; Lever *et al.* 2015), but one that is vital when there is insufficient energy for growth.

IMPLICATIONS FOR ANAEROBIC METHANE OXIDATION

The methane produced by methanogens disappears in the SMTZ (Egger, Riedinger and Mogollón 2018), where the energy yield from anaerobic oxidation of methane (AOM) is much lower than that from methanogenesis (Valentine 2011). The reaction is thus thought to be energetically coupled to a syntrophic partner, such as a sulfate reducer, in cases studied so far (Holler *et al.* 2011). But if the conversion of fermented cell mass to methanogen cell
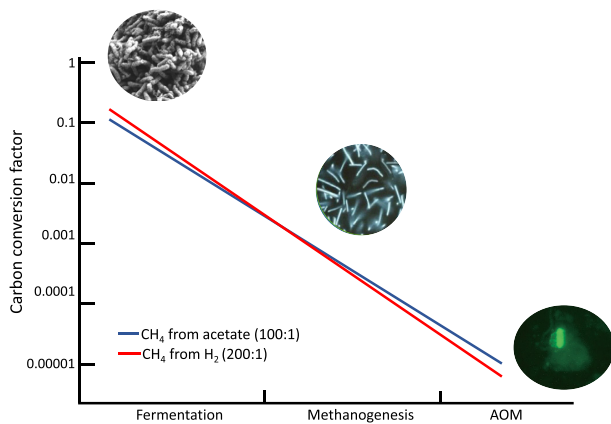
Figure 3. Estimated carbon conversion factors for metabolic feeding chains in subseafloor anoxic sediments. Cartoon schematic showing the decreasing carbon conversion from the base of the microbial food chain (fermentation) to methanogenesis, and AOM. This explains the global exponential decline in biomass with increasing depth in anoxic sediment (Fig. 3). Photographs of methanogens and the single AOM (ANME) cell are modified from Karl Stetter, and Lloyd, Alperin and Teske (2011), respectively. The image of the fermenters is the author's (W. Orsi) own work.

mass occurs at a ratio of 100:1 (20:1 if unfermented amino acids are assimilated with H_2-dependent ATP synthesis), the subsequent anaerobic conversion of methane to cell mass via AOM can hardly be better. We can briefly consider the possibility of biomass accumulation via anaerobic methane oxidation. Unfortunately, at the time of writing, balanced stoichiometric reactions including a carbon balance for cells that employ anaerobic methane oxidation are not available. However, in one example where anaerobic methane oxidation was studied in laboratory cultures, the methane oxidizing cells were acting as autotrophs, incorporating labeled CO_2, as opposed to incorporating labeled methane (Milucka *et al.* 2012) or amino acids. The energy yield for AOM is lower than that for methanogenesis (Holler *et al.* 2011). That means that the biomass conversion ratio for AOM cannot be higher than for methanogenesis, placing a very generous upper bound on the carbon conversion ratio at one CO_2 fixed as cell mass per 20 methane oxidized (the methanogen ratio). The ~10–100-fold longer doubling times for AOM, combined with the circumstance that the ATP costs for amino acid biosynthesis will be the same for autotrophic growth during AOM (Milucka *et al.* 2012) as for methanogenesis, suggest that the overall carbon conversion ratio from methanogenesis to AOM will be on the order of 100 methane oxidized per carbon fixed as anaerobic methane oxidizing archaeon (ANME) cell mass. This corresponds to a cell mass conversion ratio from fermentation to ANME via methanogenesis on the order of 10 000:1 (Fig. 3). This probably explains why the activity and abundance of ANME populations is so low in subseafloor settings, compared to methane seeps at the surface (Orsi 2018).

Preserved consortia of anaerobic methane oxidizing ANME cells with sulfate-reducing bacteria in close physical contact (that is, cells that were evidently growing together) are typically enriched in methane seeps, like those on the continental shelf break and in the Black Sea (Knittel *et al.* 2005). However, in deep anoxic sediment where the SMTZ can lie down to 30 m below the seafloor (D'Hondt *et al.* 2003), our calculations suggest that anaerobic oxidation of methane does not represent a successful strategy for growth, because it has a carbon conversion factor from fermentation at roughly 1:10 000 (Fig. 3). This fits with

the observations from sampling of such deep biosphere environments, as, to our knowledge, no photographic evidence of preserved ANME-sulfate reducing bacteria consortia similar to those observed at methane seeps have been reported from deep anoxic sediments, specifically in the deep SMTZs. Rather, the ANME cells observed are often found in isolation (Lloyd, Alperin and Teske 2011). In deep anoxic sediment, it is thus possible that the ANME are living as methanogens, rather than as anaerobic methane oxidizers (Lloyd, Alperin and Teske 2011; Beulig *et al.* 2019).

Recent studies point to the possibility of iron reduction coupled to the anaerobic oxidation of methane in anoxic sediments. At cold methane seeps, ANME cells can oxidize methane with Fe oxides at the sediment surface (Scheller *et al.* 2016). Vigderovich *et al.* (2019) reported iron reduction in methanogenic sediment down to a depth of 5 m in the Mediterranean. Bar-Or *et al.* (2017) reported slurry cultures that reduce Fe oxides and oxidize methane, but the partners and pathways involved have not been characterized. Egger *et al.* (2017) suggested that iron oxide reduction might affect sediments subject to changes in organic matter loading, but very deep sediment that we are discussing here is isolated from changes in organic matter loading. Riedinger *et al.* (2014) suggested that methane oxidation coupled to Fe oxides and Mn(IV) reduction at depths down to 8 m are important in sediments characterized by rapid deposition and that are rich in manganese and iron oxides in the methanogenic zone. Slomp *et al.* (2013) also suggested a role for methane oxidation coupled to Fe oxides and Mn(IV) reduction in surface sediments down to a depth of 40 cm. The biological process of iron oxide-dependent methane oxidation is thought to require 8 atoms of Fe oxides for each methane oxidized (Riedinger *et al.* 2014). Although it cannot be excluded that Fe oxides and/or Mn(IV)-dependent methane oxidation occurs in deep sediments, we note that the activity and abundance of ANME populations is very low in subseafloor settings, as opposed to shallow sediment or methane seeps at the surface where ANME tends to be more abundant with higher activity (Orsi 2018). Accordingly, it is unlikely that ANME-mediated Fe oxides and Mn(IV)-dependent methane oxidation play a substantial role in deep sediment carbon conversion.

EVIDENCE FOR A LOW-TEMPERATURE LIFE–DEATH TRANSITION ZONE (LDTZ)

Our analysis suggests that the steadily decreasing ATP budgets and subsequent carbon transfer efficiencies for protein biosynthesis that result primarily from amino acid fermentations should eventually represent an insurmountable barrier for life in ultradeep subseafloor anoxic sediment at low temperatures (<120°C). This potential LDTZ would represent a transition from the last biologically catalyzed life processes to catalyzed processes that are no longer coupled to life. While a low-temperature (<120°C) LDTZ has never been observed in anoxic sediment, the deepest report of subseafloor life is 2.5 km below the seafloor where the detection limit for life was already close to being reached at roughly one cell per cubic centimeter of sediment or below detection (Inagaki *et al.* 2015; Fig. 4). The temperatures at the deepest depths were between 40 and 60°C (Heuer *et al.* 2016), and thus the apparent lack of subseafloor life at 2500 m below seafloor (mbsf) cannot be explained by high temperature. Thus, Inagaki *et al.* (2015) apparently sampled the beginnings of a low-temperature LDTZ that our physiological calculations predict.
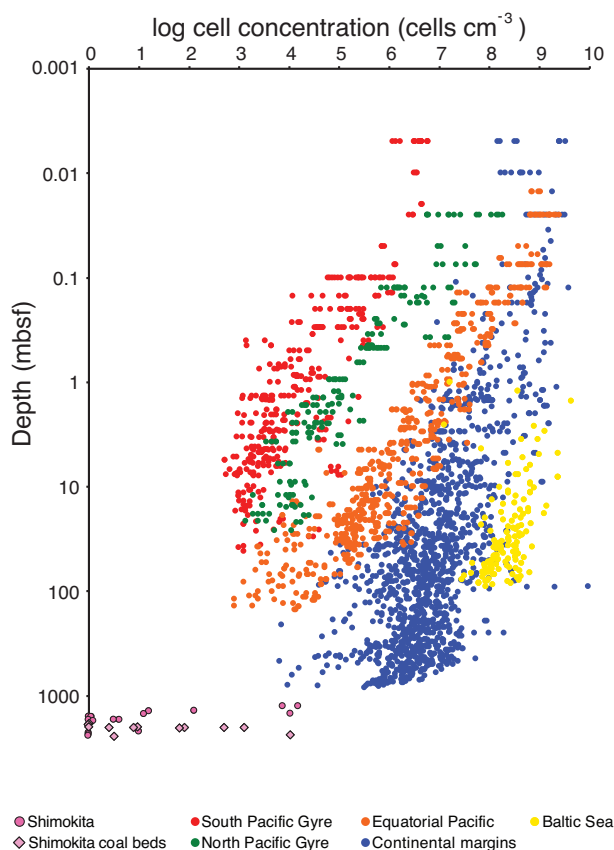
Figure 4. Global distribution of microbial biomass in subseafloor sediments. Data are replotted from Kallmeyer *et al.*, with cell counts from the more recent Shimokita (Inagaki *et al.* 2015) and the Baltic Sea (Andren *et al.* 2015) deep drilling expeditions. Note that the global regression line changes at ~500 mbsf for continental margins, and at ~75 mbsf for equatorial Pacific sites, whereby the rate of cell death increases after dropping below 10^5 cells cm^{-3}. Mbsf: meters below seafloor.

Below subseafloor depths of 2 km, life was below detection except for intervals that had elevated organic matter contents from ancient coal (Inagaki *et al.* 2015). Thus, organic matter availability is indeed a most critical factor that constrains the depth of a potential low-temperature LDTZ. This fits with our physiologically based estimate that posits fermentation of organic substrates ultimately to control the size of the deep anoxic subseafloor biosphere. Geochemical data from samples taken in the deepest deep biosphere suggested that hydrogenotrophic CO_2-reducing methanogenesis was the predominant pathway for methane formation, as opposed to acetoclastic methanogenesis (Inagaki *et al.* 2015). This is also consistent with our calculations, which indicate that the biomass conversion from hydrogenotrophic methanogenesis is two times lower than that for acetoclastic methanogenesis.

Looking at the compiled data (Fig. 3), an inflection point is reached when the cell counts drop below a critical cell concentration of 10^5–10^6 cells cm^{-3} (Fig. 4) indicating that the distance between cells results in an increased rate of cell death. Indeed, because the time required for chemical diffusion is proportional to the square of diffusion distance, the metabolization rate must decline exponentially with increasing distance between sources and sinks of organic matter (D'Hondt *et al.* 2019): dead and living cells, respectively. This increase in cell death rate below a cell concentration of 10^5 cells cm^{-3} can be partly explained by the

physiological limits to life that we calculate here. Since the primary fermentable substrates are necromass (amino acids) from other microbes, once the cell density of microbes reaches a critical threshold of $<10^5$ cells cm^{-3} the rate of cell death increases (Fig. 4), presumably due to less organic matter from recently deceased cells becoming available to living fermenters.

With the exception of hydrothermal sediments, the geothermal gradient within the upper 100 km of the Earth is usually ~30°C/km (Earle 2015). However, the slope of the geothermal gradient is controlled by the heat flux from the underlying crust, the temperature at the sediment–water interface and the thermal conductivity of the sediments (Stranne and O'Regan 2015). Thus, the geothermal gradient can in some instances be as low as 15°C/km (Earle 2015) such as in the Gulf of Mexico where sediments are 10 km thick (Straume *et al.* 2019) and exhibit a wide range of thermal gradient strength from 15 to 50°C/km (Christie and Nagihara 2016). If the sediments with a 15°C/km geothermal gradient also exhibit an LDTZ below ~2500 mbsf as indicated in Japanese shelf sediments (Inagaki *et al.* 2015), the 'low-temperature' (40–120°C) abiotic zone could extend from 2.5 km to the 120°C isotherm several kilometers deeper below. This abiotic zone would not be due to high temperature, but rather to the depletion of fermentable organic matter to concentrations that no longer meet the minimal energy requirement of a cell.

The total volume of subseafloor sediment habitats cooler than 120°C is immense and estimated to be 2.6×10^8 km^3 (LaRowe *et al.* 2017; D'Hondt *et al.* 2019). However, if 80°C is taken as the major thermal barrier for subseafloor life, then this habitable area would be restricted (LaRowe *et al.* 2017). The high-temperature limit to oil and gas biodegradation (Head, Jones and Larter 2003) is 80–90°C, which is considerably lower than the high-temperature limit to life determined in experiments using methanogenic archaea grown under energy- and nutrient-rich conditions (Takai *et al.* 2008) at 122°C. Thus, the high-temperature limit to life may vary from one environment to another as a function of bioavailable energy flux or nutrients. The high-temperature limit to life in the subseafloor is currently unknown but is an area of active investigation through the recent IODP Expedition 370 'Temperature Limit of the Deep Biosphere off Muroto' (Heuer *et al.* 2016). The results of that expedition will surely have important implications for the effect of high, and potentially low-temperature LDTZs.

POTENTIAL CHEMICAL REACTIONS BELOW AN LDTZ

Where life tapers out, the only possible chemical reactions that remain are abiotic. The most likely chemical reactions no longer coupled to life below the LDTZ are those that are exergonic with a non-zero rate (Fig. 5). These include peptide hydrolysis and nucleic acid hydrolysis whereby RNA would be more affected than DNA. Additional purely chemical reactions would be amino acid racemization and sugar decay. Bacterial lipids are mainly esters of long chain fatty acids, the ester bonds of which are readily hydrolyzed in marine sediments (Xie *et al.* 2013). Archaeal lipids on the other hand are ethers that are much better preserved in anoxic marine sediments (Xie *et al.* 2013), and should be more stable below the LDTZ. Radiolysis of water results in the abiotic formation of H_2 in deep marine sediments that could be a potential energy source (Dzaugis *et al.* 2016). Cellular activity might result from H_2 derived purely from radiolysis of water. Genes encoding hydrogenase proteins involved in the potential oxidation of H_2 have been found in deep subseafloor clays
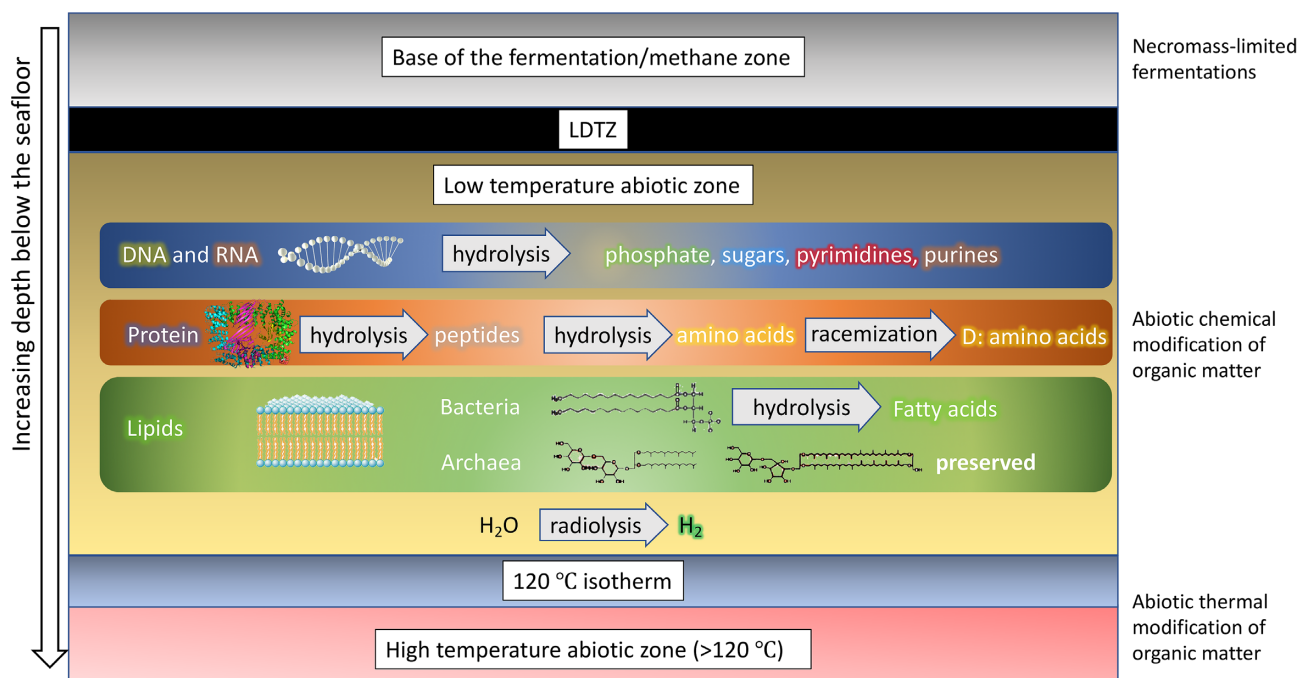
Figure 5. Potential abiotic chemical reactions taking place below the LDTZ.

supporting a possible utilization of H_2 derived from radiolysis by subseafloor life (Vuillemin et al. 2019). Abiotic radiolysis of water might also play a role in controlling the depth of the LDTZ by supplying H_2 as an energy source to H_2-utilizing microbes (methanogens) above the LDTZ.

CONCLUSION

Fermentation in anoxic sediment is not primary production; it is terminal disproportionation. The aim of this work is not to calculate exact biomass conversion rates, but to get an order of magnitude estimate on their trends based on the estimated availability of relevant substrates in the methane zone of anoxic subseafloor sediment. Our analysis indicates that fermentation in deep anoxic sediment is a kind of swan song—a farewell to the active biosphere and a transition into the death and long-term stationary phases of microbial life. From the standpoint of metabolism, life likely started on Earth as H_2-CO_2 dependent reactions giving rise to autotrophic acetogens and methanogens as the first free living cells (Weiss et al. 2016; Varma et al. 2018; Muchowska, Varma and Moran 2019). Fermentations of amino acids and bases were probably the first form of heterotrophic metabolism on Earth because cell substance is an excellent growth substrate and because carbon compounds from space are mostly unfermentable and structurally too heterogeneous to support a metabolism (Schönheit et al. 2016). Looking forward in time, fermentations in anoxic sediments might end up being the last form of metabolism on Earth. By injecting carbon source substrates and terminal acceptors into sediment and monitoring growth or gene expression, it should be possible to identify factors limiting life near the LDTZ.

Conflicts of Interests. None declared.

REFERENCES

Adams MW, Kelly RM. Thermostability and thermoactivity of enzymes from hyperthermophilic Archaea. *Bioorg Med Chem* 1994;**2**:659–67.

Allison ME, Bryant MP. Biosynthesis of branched-chain amino acids from branched-chain fatty acids by rumen bacteria. *Arch Biochem Biophys* 1963;**101**:269–77.

Andreesen JR. Glycine reductase mechanism. *Curr Opin Chem Biol* 2004;**8**:454–61.

Andren T, Jørgensen BB, Cotterill C et al. IODP expedition 347: Baltic Sea basin paleoenvironment and biosphere. *Sci Drill* 2015;**20**:1–12.

Angenent LT, Richter H, Buckel W et al. Chain elongation with reactor microbiomes: open-culture biotechnology to produce biochemicals. *Environ Sci Technol* 2016;**50**:2796–810.

Aono R, Sato T, Imanaka T et al. A pentose bisphosphate pathway for nucleoside degradation in Archaea. *Nat Chem Biol* 2015;**11**:355–60.

Bar-Or I, Elvert M, Eckert W et al. Anaerobic oxidation of methane performed by a mixed bacterial–archaeal community based on poorly reactive minerals. *Environ Sci Technol* 2017;**51**:12293–301.

Barker HA. Amino acid degradation by anaerobic bacteria. *Annu Rev Biochem* 1981;**50**:23–40.

Barker SA, Brimacombe JS, How MJ et al. Two new amino-sugars from an antigenic polysaccharide of Pneumococcus. *Nature* 1961;**189**:303–4.

Beulig F, Roy H, Glombitza C et al. Control on rate and pathway of anaerobic organic carbon degradation in the seabed. *Proc Natl Acad Sci USA* 2018;**115**:367–72.

Beulig F, Roy H, McGlynn SE et al. Cryptic CH_4 cycling in the sulfate-methane transition of marine sediments apparently mediated by ANME-1 archaea. *ISME J* 2019;**13**:250–62.

Bird JT, Tague E, Zinke L *et al*. Uncultured microbial phyla suggest mechanisms for multi-thousand-year subsistence in Baltic Sea sediments. *mBio* 2019;**10**:e02376–18.

Bowles MW, Mogollon J, Kasten S *et al*. Global rates of marine sulfate reduction and implications for sub-sea-floor metabolic activities. *Science* 2014;**344**:889–91.

Brasen C, Esser D, Rauch B *et al*. Carbohydrate metabolism in Archaea: current insights into unusual enzymes and pathways and their regulation. *Microbiol Mol Biol Rev* 2014;**78**: 89–175.

Braun S, Mhatre SS, Jaussi M *et al*. Microbial turnover times in the deep seabed studied by amino acid racemization modelling. *Sci Rep* 2017;**7**:5680.

Buckel W, Barker HA. Two pathways of glutamate fermentation by anaerobic bacteria. *J Bacteriol* 1974;**117**:1248–60.

Buckel W, Miller SL. Equilibrium constants of several reactions involved in the fermentation of glutamate. *Eur J Biochem* 1987;**164**:565–9.

Buckel W, Thauer RK. Energy conservation via electron bifurcating ferredoxin reduction and proton/Na$^+$ translocating ferredoxin oxidation. *Biochim Biophys Acta* 2013;**1827**:94–113.

Buckel W, Thauer RK. Flavin-based electron bifurcation, a new mechanism of biological energy coupling. *Chem Rev* 2018;**118**:3862–86.

Buckel W. Unusual enzymes involved in five pathways of glutamate fermentation. *Appl Microbiol Biotechnol* 2001;**57**:263–73.

Burdige DJ. Dissolved carbohydrates in interstitial waters from the equatorial Pacific and Peru margin, ODP Leg 201. In: Jørgensen BB, D'Hondt SJ, Miller DJ , (eds). *Proceedings of the Ocean Drilling Program*, Vol. 201. 2006, 1–10.

Burdige DJ. Sediment pore waters. In: Hansell DA, Carlson CA , (eds). *Biogeochemistry of Marine Dissolved Organic Matter*. USA: Elsevier Inc., 2002, 611–63.

Christie CH, Nagihara S. Geothermal gradients of the northern continental shelf of the Gulf of Mexico. *Geosphere* 2016;**12**: 26–34.

D'Hondt S, Jørgensen BB, Miller DJ *et al*. Distributions of microbial activities in deep subseafloor sediments. *Science* 2004;**306**:2216–21.

D'Hondt S, Jørgensen BB, Miller DJ *et al*. Site 1229. Proceedings of the Ocean Drilling Program, Initial Reports. Texas A&M University, College Station, TX 77845-9547. 2003.

D'Hondt S, Pockalny R, Fulfer VM *et al*. Subseafloor life and its biogeochemical impacts. *Nat Commun* 2019;**10**:3519.

Daniel SL, Keith ES, Yang H *et al*. Utilization of methoxylated aromatic compounds by the acetogen *Clostridium thermoaceticum*: expression and specificity of the co-dependent O-demethylating activity. *Biochem Biophys Res Commun* 1991;**180**:416–22.

Dzaugis ME, Spivack AJ, Dunlea AG *et al*. Radiolytic hydrogen production in the subseafloor basaltic aquifer. *Front Microbiol* 2016;**7**:76.

Earle S. The temperature of Earth's interior. *Physical Geology*. BCcampus: Victoria, BC. 2015.

Egger M, Hagens M, Sapart CJ *et al*. Iron oxide reduction in methane-rich deep Baltic Sea sediments. *Geochim Cosmochim Acta* 2017;**207**:256–76.

Egger M, Riedinger N, Mogollón MJ. Global diffusive fluxes of methane in marine sediments. *Nat Geosci* 2018;**11**:421–5.

Elkins JG, Podar M, Graham DE *et al*. A korarchaeal genome reveals insights into the evolution of the Archaea. *Proc Natl Acad Sci USA* 2008;**105**:8102–7.

Engelhardt T, Kallmeyer J, Cypionka H *et al*. High virus-to-cell ratios indicate ongoing production of viruses in deep subsurface sediments. *ISME J* 2014;**8**:1503–9.

Finkel SE. Long-term survival during stationary phase: evolution and the GASP phenotype. *Nat Rev Microbiol* 2006;**4**:113–20.

Fonknechten N, Chaussonnerie S, Tricot S *et al*. *Clostridium sticklandii*, a specialist in amino acid degradation: revisiting its metabolism through its genome sequence. *BMC Genomics* 2010;**11**:555.

Glombitza C, Egger M, Roy H *et al*. Controls on volatile fatty acid concentrations in marine sediments (Baltic Sea). *Geochim Cosmochim Acta* 2019;**258**:226–41.

Hartwich K, Poehlein A, Daniel R. The purine-utilizing bacterium *Clostridium acidurici* 9a: a genome-guided metabolic reconsideration. *PLoS One* 2012;**7**:e51662.

Head IM, Jones DM, Larter SR. Biological activity in the deep subsurface and the origin of heavy oil. *Nature* 2003;**426**:344–52.

Herrmann G, Jayamani E, Mai G *et al*. Energy conservation via electron-transferring flavoprotein in anaerobic bacteria. *J Bacteriol* 2008;**190**:784–91.

Heuer VB, Inagaki F, Morono Y *et al*. Expedition 370 preliminary report: temperature limit of the deep biosphere off Muroto. *International Ocean Discovery Program* 2016. http://dx.doi.org/10.14379/iodp.pr.370.2017.

He Y, Li M, Perumal V *et al*. Genomic and enzymatic evidence for acetogenesis among multiple lineages of the archaeal phylum Bathyarchaeota widespread in marine sediments. *Nat Microbiol* 2016;**1**:16035.

Hoehler TM, Jørgensen BB. Microbial life under extreme energy limitation. *Nat Rev Microbiol* 2013;**11**:83–94.

Holler T, Wegener G, Niemann H *et al*. Carbon and sulfur back flux during anaerobic microbial oxidation of methane and coupled sulfate reduction. *Proc Natl Acad Sci USA* 2011;**108**:E1484–1490.

Holmkvist L, Ferdelman T, Jørgensen BB. A cryptic sulfur cycle driven by iron in the methane zone of marine sediment (Aahurs Bay, Denmark). *Geochim Cosmochim Acta* 2011;**75**:3581–99.

Imachi H, Nobu MK, Nakahara N *et al*. Isolation of an archaeon at the prokaryote–eukaryote interface. *Nature* 2020;**577**:519–25.

Inagaki F, Hinrichs KU, Kubo Y *et al*. Exploring deep microbial life in coal-bearing sediment down to ~2.5 km below the ocean floor. *Science* 2015;**349**:420–4.

Kallmeyer J, Pockalny R, Adhikari RR *et al*. Global distribution of microbial abundance and biomass in subseafloor sediment. *Proc Natl Acad Sci USA* 2012;**109**:16213–6.

Kaster A, Blackwell-Mayer K, Pasarell B *et al*. Single cell study of Dehalococcoidetes species from deep-sea sediments of the Peruvian Margin. *ISME J* 2014;**8**:1831–42.

Katayama T, Nobu MK, Kusada H *et al*. Membrane-bounded nucleoid discovered in a cultivated bacterium of the candidate phylum 'Atribacteria'. *bioRxiv* 2019. dx.doi.org/10.1101/728279.

Knittel K, Losekann T, Boetius A *et al*. Diversity and distribution of methanotrophic archaea at cold seeps. *Appl Environ Microb* 2005;**71**:467–79.

LaRowe DE, Amend JP. The energetics of fermentation in natural settings. *Geomicrobiol J* 2019;**36**:1–14.

LaRowe DE, Burwicz E, Arndt S *et al*. Temperature and volume of global marine sediments. *Geology* 2017;**45**:275–8.

Lengeler JW, Drews G, Schegel HG. *Biology of the Prokaryotes*. USA: Blackwell Science, 1999.

Lens PN, Dijkema C, Stams AJ. 13C-NMR study of propionate metabolism by sludges from bioreactors treating sulfate and sulfide rich wastewater. *Biodegradation* 1998;**9**:179–86.

Lever MA, Heuer VB, Morono Y *et al.* Acetogenesis in deep subseafloor sediments of the Juan de Fuca Ridge Flank: a synthesis of geochemical, thermodynamic, and gene-based evidence. *Geomicrobiol J* 2009;**27**:183–211.

Lever MA, Rogers KL, Lloyd KG *et al.* Life under extreme energy limitation: a synthesis of laboratory- and field-based investigations. *FEMS Microbiol Rev* 2015;**39**:688–728.

Lever MA. Acetogenesis in the energy-starved deep biosphere - a paradox? *Front Microbiol* 2012;**2**:284.

Lin YS, Heuer VB, Goldhammer T *et al.* Towards constraining H2 concentrations in subseafloor sediment: a proposal for combined analysis by two distinct approaches. *Geochim Cosmochim Acta* 2012;**77**:186–201.

Lloyd KG, Alperin MJ, Teske A. Environmental evidence for net methane production and oxidation in putative ANaerobic MEthanotrophic (ANME) archaea. *Environ Microbiol* 2011;**13**:2548–64.

Lloyd KG, Schreiber L, Petersen DG *et al.* Predominant archaea in marine sediments degrade detrital proteins. *Nature* 2013;**496**:215–8.

Lomstein BA, Langerhuus AT, D'Hondt S *et al.* Endospore abundance, microbial growth and necromass turnover in deep sub-seafloor sediment. *Nature* 2012;**484**:101–4.

Martin WF, Neukirchen S, Zimorski V *et al.* Energy for two: new archaeal lineages and the origin of mitochondria. *Bioessays* 2016;**38**:850–6.

Milucka J, Ferdelman TG, Polerecky L *et al.* Zero-valent sulphur is a key intermediate in marine methane oxidation. *Nature* 2012;**491**:541–6.

Montag D, Schink B. Formate and hydrogen as electron shuttles in terminal fermentations in an oligotrophic freshwater lake sediment. *Appl Environ Microb* 2018;**84**:e01572–18.

Muchowska KB, Varma SJ, Moran J. Synthesis and breakdown of universal metabolic precursors promoted by iron. *Nature* 2019;**569**:104–7.

Møller MH, Glombitza C, Lever MA *et al.* D:L-amino acid modeling reveals fast microbial turnover of days to months in the subsurface hydrothermal sediment of Guaymas Basin. *Front Microbiol* 2018;**9**:967.

Müller N, Griffin BM, Stingl U *et al.* Dominant sugar utilizers in sediment of Lake Constance depend on syntrophic cooperation with methanogenic partner organisms. *Environ Microbiol* 2008;**10**:1501–11.

Müller V, Chowdhury NP, Basen M. Electron bifurcation: a long-hidden energy-coupling mechanism. *Annu Rev Microbiol* 2018;**72**:331–53.

Müller V. *Bacterial Fermentation*. Chichester, UK: John Wiley & Sons Ltd, 2008.

Neidhardt FC, Ingraham JL, Schaecter M. *Physiology of the Bacterial Cell*. Sunderland, MA: Sinauer Associates, 1990.

Nobu MK, Dodsworth JA, Murugapiran SK *et al.* Phylogeny and physiology of candidate phylum 'Atribacteria' (OP9/JS1) inferred from cultivation-independent genomics. *ISME J* 2016;**10**:273–86.

Orsi WD, Edgcomb V, Christman G *et al.* Gene expression in the deep biosphere. *Nature* 2013;**499**:205–8.

Orsi WD, Vuillemin A, Rodriguez P *et al.* Metabolic activity analyses demonstrate that Lokiarchaeon exhibits homoacetogenesis in sulfidic marine sediments. *Nat Microbiol* 2019;**5**: 248–55.

Orsi WD. Ecology and evolution of seafloor and subseafloor microbial communities. *Nat Rev Microbiol* 2018;**16**:671–83.

Parkes RJ, Cragg BA, Wellsbury P. Recent studies on bacterial populations and processes in subseafloor sediments: a review. *Hydrogeol J* 2000;**8**:11–28.

Parkes RJ, Webster G, Cragg BA *et al.* Deep sub-seafloor prokaryotes stimulated at interfaces over geological time. *Nature* 2005;**436**:390–4.

Plugge CM, van Leeuwen JM, Hummelen T *et al.* Elucidation of the pathways of catabolic glutamate conversion in three thermophilic anaerobic bacteria. *Arch Microbiol* 2001;**176**: 29–36.

Riedinger N, Formolo MJ, Lyons TW *et al.* An inorganic geochemical argument for coupled anaerobic oxidation of methane and iron reduction in marine sediments. *Geobiology* 2014;**12**:172–81.

Scheller S, Yu H, Chadwick GL *et al.* Artificial electron acceptors decouple archaeal methane oxidation from sulfate reduction. *Science* 2016;**351**:703–7.

Schink B. Energetics of syntrophic cooperation in methanogenic degradation. *Microbiol Mol Biol Rev* 1997;**61**:262–80.

Schlegel K, Welte C, Deppenmeier U *et al.* Electron transport during aceticlastic methanogenesis by *Methanosarcina acetivorans* involves a sodium-translocating Rnf complex. *FEBS J* 2012;**279**:4444–52.

Schuchmann K, Müller V. Energetics and application of heterotrophy in acetogenic bacteria. *Appl Environ Microb* 2016;**82**:4056–69.

Schut GJ, Adams MW. The iron-hydrogenase of *Thermotoga maritima* utilizes ferredoxin and NADH synergistically: a new perspective on anaerobic hydrogen production. *J Bacteriol* 2009;**191**:4451–7.

Schönheit P, Buckel W, Martin WF. On the origin of heterotrophy. *Trends Microbiol* 2016;**24**:12–25.

Schönheit P, Moll J, Thauer RK. Growth parameters (Ks, μmax, Ys) of *Methanobacterium thermoautotrophicum*. *Arch Microbiol* 1980;**127**:59–65.

Scott JW, Poole FL, Adams MW. Characterization of ten heterotetrameric NDP-dependent acyl-CoA synthetases of the hyperthermophilic archaeon *Pyrococcus furiosus*. *Archaea* 2014;**2014**:176863.

Sewell HL, Kaster AK, Spormann AM. Homoacetogenesis in deep-sea chloroflexi, as inferred by single-cell genomics, provides a link to reductive dehalogenation in terrestrial dehalococcoidetes. *mBio* 2017;**8**:e02022–17.

Slomp CP, Mort HP, Jilbert T *et al.* Coupled dynamics of iron and phosphorus in sediments of an oligotrophic coastal basin and the impact of anaerobic oxidation of methane. *PLoS One* 2013;**8**:e62386.

Smith EA, Macfarlane GT. Formation of phenolic and indolic compounds by anaerobic bacteria in the human large intestine. *Microb Ecol* 1997;**33**:180–8.

Stouthamer AH. A theoretical study on the amount of ATP required for synthesis of microbial cell material. *Antonie Van Leeuwenhoek* 1973;**39**:545–65.

Stouthamer AH. The search for correlation between theoretical and experimental growth yields. In: Quayle JR (ed.). *International Reviews of Biochemistry, Microbial Biochemistry*. Baltimore: University Park Press. 1979.

Stranne C, O'Regan M. Conductive heat flow and nonlinear geothermal gradients in marine sediments - observations from Ocean Drilling Program boreholes. *Geo-Mar Lett* 2015;**36**:1–9.

Straume EO, Gaina C, Medvedev S *et al*. GlobSed: updated total sediment thickness in the world's oceans. *Geochem Geophys Geosyst* 2019;**20**:1756–72.

Takai K, Nakamura K, Toki T *et al*. Cell proliferation at 122 degrees C and isotopically heavy CH_4 production by a hyperthermophilic methanogen under high-pressure cultivation. *Proc Natl Acad Sci USA* 2008;**105**:10949–54.

Thauer RK, Jungermann K, Decker K. Energy conservation in chemotrophic anaerobic bacteria. *Bacteriol Rev* 1977;**41**: 100–80.

Thauer RK, Kaster AK, Seedorf H *et al*. Methanogenic archaea: ecologically relevant differences in energy conservation. *Nat Rev Microbiol* 2008;**6**:579–91.

Valentine DL. Emerging topics in marine methane biogeochemistry. *Ann Rev Mar Sci* 2011;**3**:147–71.

Varma SJ, Muchowska KB, Chatelain P *et al*. Native iron reduces CO2 to intermediates and end-products of the acetyl-CoA pathway. *Nat Ecol Evol* 2018;**2**:1019–24.

Vigderovich H, Liang L, Herut B *et al*. Evidence for microbial iron reduction in the methanic sediments of the oligotrophic southeastern Mediterranean continental shelf. *Biogeosciences* 2019;**16**:3165–81.

Vuillemin A, Wankel SD, Coskun OK *et al*. Archaea dominate oxic subseafloor communities over multimillion-year time scales. *Sci Adv* 2019;**5**:eaaw4108.

Weiss MC, Sousa FL, Mrnjavac N *et al*. The physiology and habitat of the last universal common ancestor. *Nat Microbiol* 2016;**1**:16116.

Welte C, Deppenmeier U. Bioenergetics and anaerobic respiratory chains of aceticlastic methanogens. *Biochim Biophys Acta* 2014;**1837**:1130–47.

Wrighton KC, Thomas BC, Sharon I *et al*. Fermentation, hydrogen, and sulfur metabolism in multiple uncultivated bacterial phyla. *Science* 2012;**337**:1661–5.

Xie S, Lipp JS, Wegener G *et al*. Turnover of microbial lipids in the deep biosphere and growth of benthic archaeal populations. *Proc Natl Acad Sci USA* 2013;**110**: 6010–4.

Yu H, Wu CH, Schut GJ *et al*. Structure of an ancient respiratory system. *Cell* 2018;**173**:1636–1649 e1616.

Zindel U, Freudenberg W, Rieth M *et al*. *Eubacterium acidaminophilum* sp. nov., a versatile amino acid-degrading anaerobe producing or utilizing H_2 or formate. *Arch Microbiol* 1988;**150**:254–66.